Catalysis Today 170 (2011) 99–109

Contents lists available at ScienceDirect

Catalysis Today

journal homepage: www.elsevier.com/locate/cattod

A mechanistic study of borohydride anodic oxidation

Kangli Wang, Juntao Lu, Lin Zhuang*

College of Chemistry and Molecular Sciences, Hubei Key Lab of Electrochemical Power Sources, Wuhan University, Wuhan 430072, China

ARTICLE INFO

Article history:
Received 15 October 2010
Received in revised form 8 December 2010
Accepted 8 December 2010
Available online 12 January 2011

Keywords:
Borohydride oxidation
Hydrogen evolution
Electrochemistry
Fuel cell
Catalysis

ABSTRACT

In direct borohydride fuel cells, the anodic oxidation of borohydride is often accompanied by hydrogen evolution which decreases the number of electrons released to the external circuit from each borohydride ion and thus lowers the Faradaic efficiency and causes safety problems. Based on the simultaneous measurements of polarization curve and hydrogen evolution for the borohydride oxidation on a number of different catalysts, a two-stage model is proposed for the anodic oxidation of borohydride, featuring a 4-electron oxidation of borohydride to form adsorbed hydrogen atoms H^*_{ads} which may then either be oxidized to water or form hydrogen molecules through water reduction, depending on the nature of catalysts and the electrode potentials. In the view of the high reducing ability of borohydride, the intermediate H^*_{ads} may have a higher energy state and therefore, it could be oxidized at potentials negative to reversible hydrogen potential (RHE). A possible approach to reach the goal of "8-electron borohydride oxidation at potentials negative to RHE" is also suggested and realized with a titanium-oxide supported Pt catalyst.

1. Introduction

Metal borohydrides have been widely used as a strong reductant in chemical reactions and extensively applied in wastewater processing, paper bleaching and pharmaceutical synthesis [1]. In 1960s, $NaBH_4$ was first tested as a fuel for fuel cells [2,3]. The interest in using metal borohydrides as a fuel for fuel cells revived in the past decades, pushed by the new wave of energy and environment concern [4–7].

Borohydride has been considered as a potential fuel for fuel cells because of high hydrogen content (7.5 wt% for saturated aqueous solution) and the convenience in storage and transportation in comparison to hydrogen gas [8,9]. In principle, borohydride can be used in either indirect or direct ways. In indirect borohydride fuel cell (IDBFC), borohydride is simply playing the role of a hydrogen carrier and hydrolyzed to produce hydrogen gas to be fed to hydrogen–oxygen (air) fuel cells. However, direct oxidation of borohydride has the potential for higher energy efficiency. It is well known that borohydride has a much more negative standard potential than hydrogen:

$$B(OH)_4^- + 4H_2O + 8e^- \leftrightarrow BH_4^- + 8OH^- \quad -1.24\,V \text{ vs. SHE} \qquad (A)$$

Combined with an oxygen electrode, the direct borohydride fuel cell (DBFC) has a theoretical electric motive force of 1.64 V, 0.41 V greater than that of hydrogen–oxygen fuel cells. The 0.41 V extra voltage makes the DBFCs very attractive, but a DBFC with higher energy conversion efficiency than the IDBFC has not been built up. The major limitation in the performance of DBFCs is the hydrogen evolution during the borohydride anodic oxidation, which not only reduces the Faradaic efficiency of DBFC but also causes safety problems. The mechanism of the hydrogen evolution during borohydride oxidation is still not well understood. Some researchers call it hydrolysis while others consider it electrochemical water reduction [10,11]. Some additives have been used to suppress the hydrogen evolution [11–14], such as sulfur thiourea [11]. However, the oxidation of borohydride is also inhibited, resulting in a large anodic polarization and low energy conversion efficiency.

In order to secure the energy conversion efficiency for a DBFC, the overall 8e oxidation of borohydride has to be realized with no hydrogen evolution at potentials more negative than the reversible hydrogen electrode potential (RHE), which can be stated as "8-electron borohydride oxidation at potentials negative to RHE", or "E_{8e} < RHE" for short. This goal seems to be an impossible mission at a glance because at potentials negative to RHE the hydrogen evolution is thermodynamically feasible. In order to answer the question whether this mission is really possible, it is necessary to study the behavior of hydrogen evolution during borohydride oxidation.

In this work, simultaneous measurements of polarization behavior and hydrogen evolution were conducted on a number of catalysts in 2 M NaOH with different concentrations of $NaBH_4$. A two-stage mechanism for the borohydride oxidation is proposed and a possible approach to reach the goal of "8e borohydride oxidation at potentials negative to RHE" is also suggested. Finally, our recent success in approaching the goal will be cited and discussed in terms of the proposed mechanism.

* Corresponding author.
E-mail address: lzhuang@whu.edu.cn (L. Zhuang).

0920-5861/$ – see front matter © 2010 Elsevier B.V. All rights reserved.
doi:10.1016/j.cattod.2010.12.023

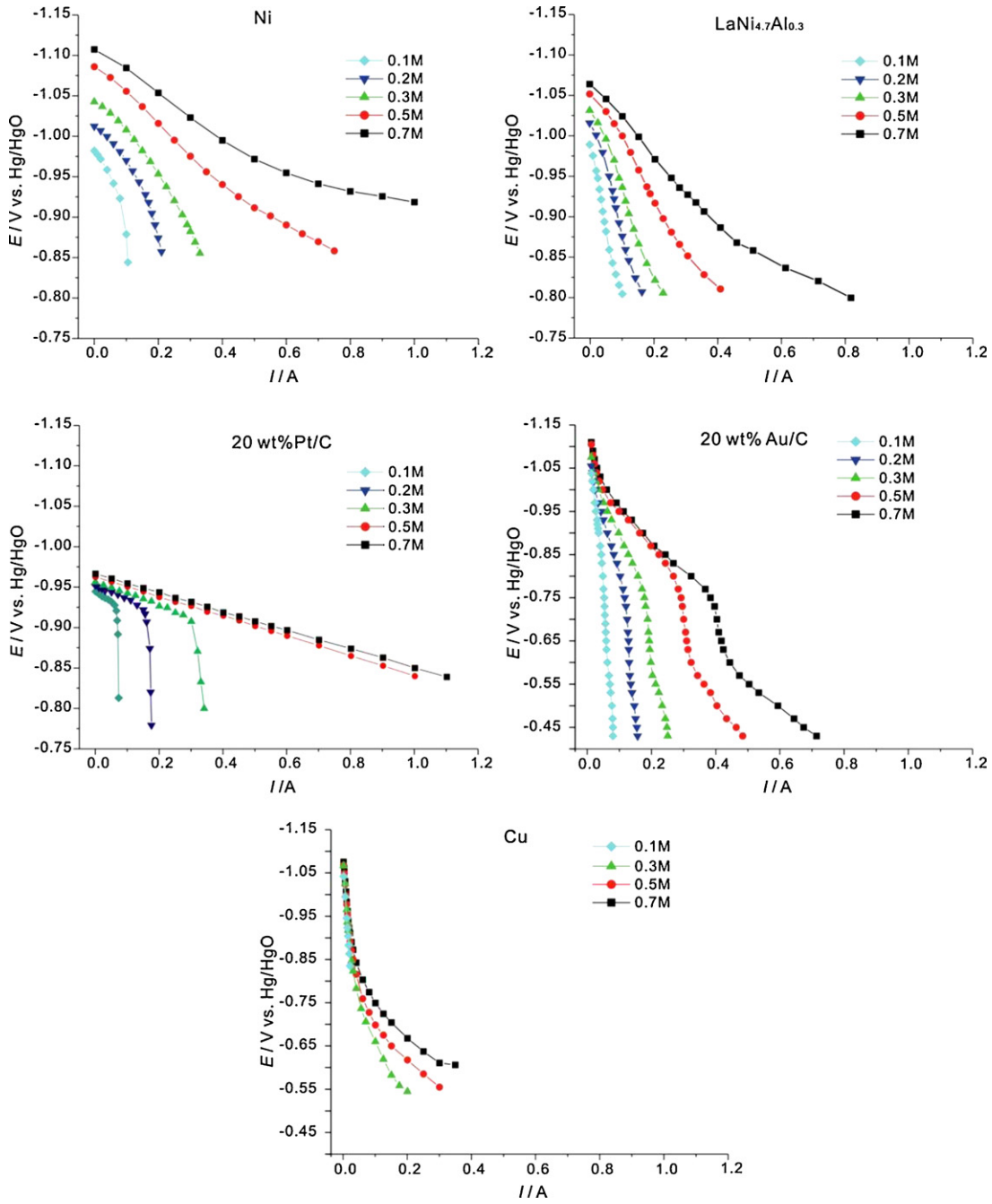

Fig. 1. Steady-state polarization curves of (a) Ni, (b) $LaNi_{4.7}Al_{0.3}$, (c) 20 wt% Pt/C, (d) 20 wt% Au/C, and (e) Cu in 2 M NaOH with different concentrations of borohydride.

2. Experimental

The experimental setup has been described in our previous paper [15]. In brief, a three-compartment cell was used. The central compartment was for the working electrode at which borohydride oxidation took place. The left and right compartments were for the counter and reference electrodes, respectively. A polymer-electrolyte membrane (quaternary ammonium polysulphone [16]) was applied to separate the neighboring compartments and to prevent convection mass transport between compartments. The central compartment was airtight and had an outlet connecting to a gas meter. The borohydride electrolyte was not artificially stirred, but disturbed by hydrogen evolution during the measurement. The reference electrode was Hg/HgO electrode in the same electrolyte (2 M NaOH). The gas evolution rate and the electric current were measured simultaneously at a series of electrode potentials controlled by a potentiostat (CHI 660, Shanghai). All measurements were carried out at room temperature.

The working electrode was made from Teflon-bound catalyst powder on a piece of nickel foam (2 cm × 2 cm in geometric area). The surfactants in the Teflon emulsion were removed by refluxing in acetone. The catalysts tested included Ni (powder, Inco 255), Cu (powder, 200 mesh, Shanghai Second Metallurgy Company), Ni-based hydrogen storage alloys (Beijing Institute of Metallurgy), carbon (XC-72) supported Pt and Au which were prepared using the impregnation-hydrogen reduction method [17].

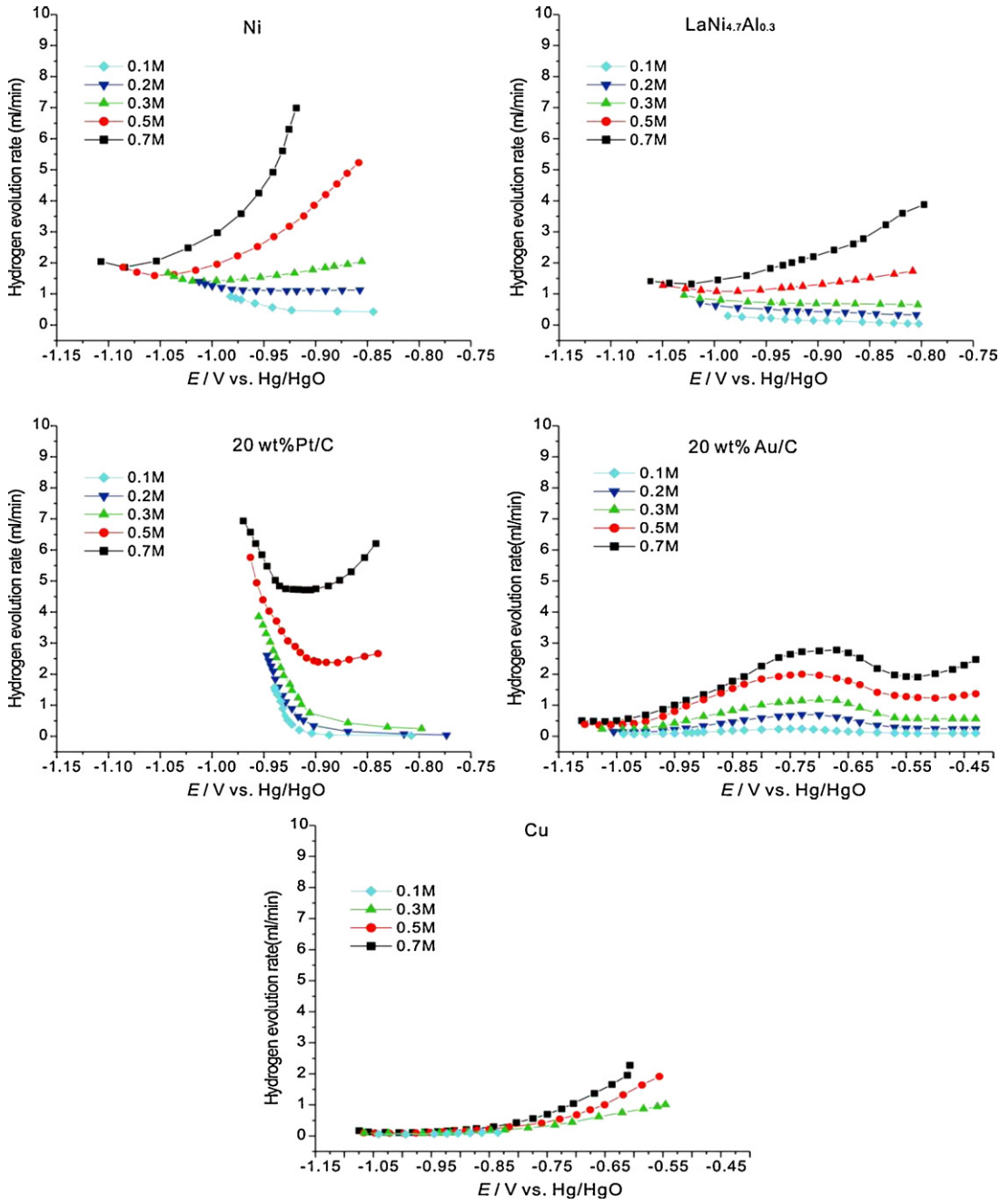

Fig. 2. Hydrogen evolution rate as a function of potential.

3. Results and discussion

3.1. Representative raw data

The representative raw data obtained from five catalysts are shown in Figs. 1–3. The open circuit potential (OCP) changes with catalysts and is believed to be a mixed potential determined by the anodic oxidation of borohydride and cathodic hydrogen evolution [15]. Among the five tested catalysts, Pt/C shows the lowest OCP, indicating a much higher activity for hydrogen evolution than that for borohydride oxidation. With increasing discharge current, electrode potential shifts to positive and the polarization increases. The characteristics of polarization curves depend strongly on the catalyst and are also influenced by the borohydride concentration, as shown in Fig. 1. A limiting currents governed by mass-transport of BH_4^- is evident on high activity catalysts, such as Pt/C, and is roughly proportional to the concentration of BH_4^-, when the concentration of borohydride is lower than 0.3 M. There is no limiting current at higher borohydride concentration, probably owing to the mass transport enhanced by hydrogen evolution. For poor catalysts like Cu, no limiting current was found in the concentration range studied. The polarization curves of Au/C show a stepwise change round −0.8 to −0.6 V probably due to surface changes, detailed discussion will not be included in this work.

Fig. 2 shows the gas evolution rate as a function of potential. The hydrogen evolution rate initially drops down and then increases steadily as the potential moves from OCP to the positive. This complication is caused by two competing processes: Increasing potential tends to suppress electrochemical hydrogen evolution (or to increase the oxidation of hydrogen), while as potential shifts

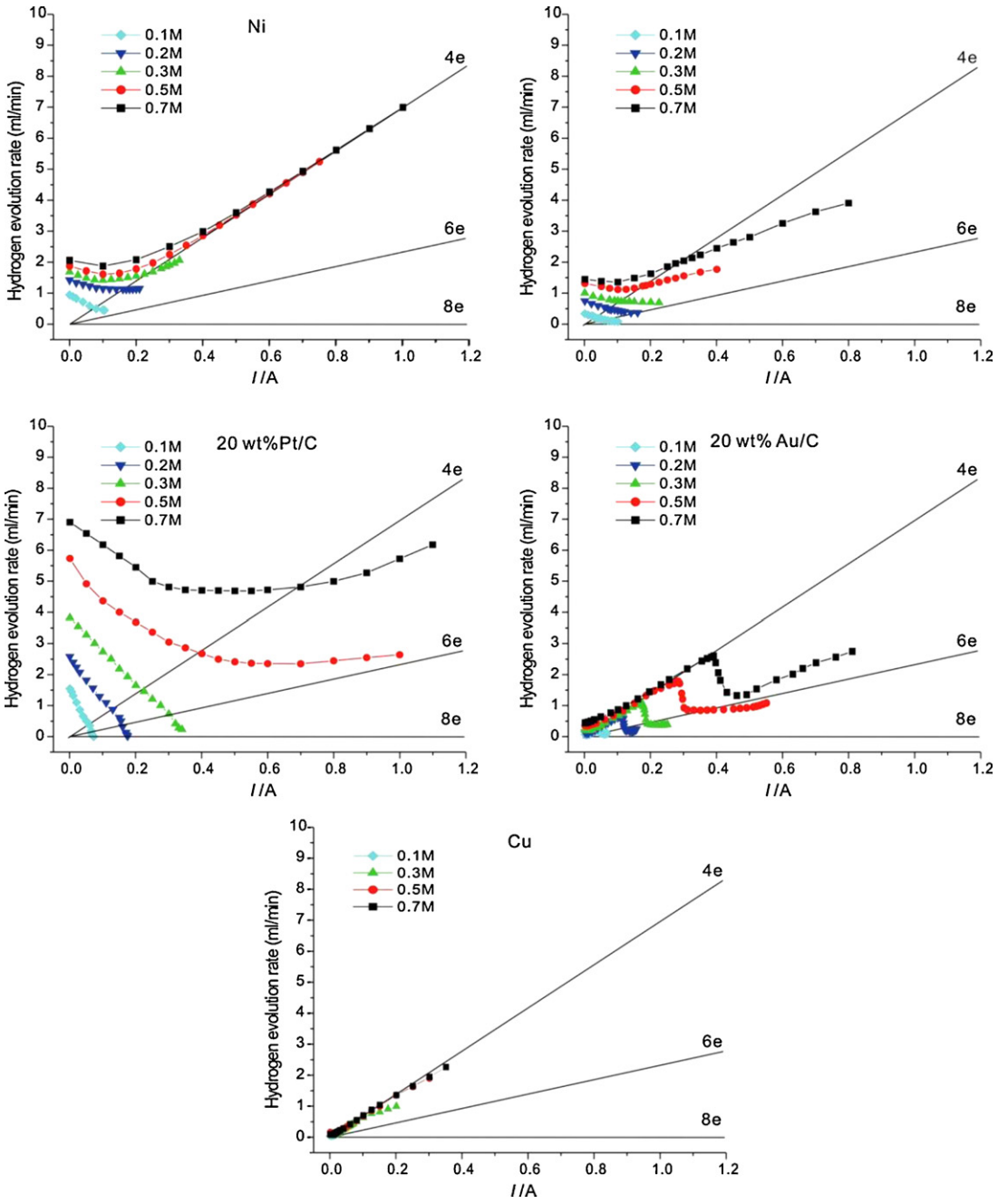

Fig. 3. Hydrogen evolution rate as a function of current.

to positive direction, the oxidation of borohydride is favorable and produces more hydrogen if the apparent electron number is less than 8.

Fig. 3 shows the correlation between the gas evolution rate and the electric current. The straight lines indicate the apparent number of electrons involved in the anodic oxidation of borohydride as defined by

$$n_{app} = \frac{8I}{G+I} \quad (1)$$

where I is the measured current and G is the current converted from hydrogen evolution rate, assuming that a hydrogen molecule accepts 2 electrons. The value $(G+I)$ represents the consumption rate of borohydride. Under open circuit condition, the measured current I is zero, $n_{app} = 0$. When $I = G$, $n_{app} = 4$. If there is no hydrogen evolution, $G = 0$, $n_{app} = 8$. As shown in Fig. 3, n_{app} changes as current and potential increase, depending on the catalyst and borohydride concentration. At lower borohydride concentrations, n_{app} increases gradually with I, while at higher borohydride concentrations, n_{app} increases first and then decreases slowly at higher currents.

The way of plotting in Fig. 3 is popular in the literature of borohydride electrochemistry [18]. The advantage of such plotting is a visual comparison between the obtained current and gas evolution rate with n_{app} ranges marked. However, this way of plotting fails to reveal the influence of electrode potential, which is of fundamental significance for electrode reactions.

3.2. n_{app} as a function of potential

Fig. 4 shows the potential dependence of n_{app} calculated using Eq. (1). For Ni and Cu, n_{app} increases with increasing potential and

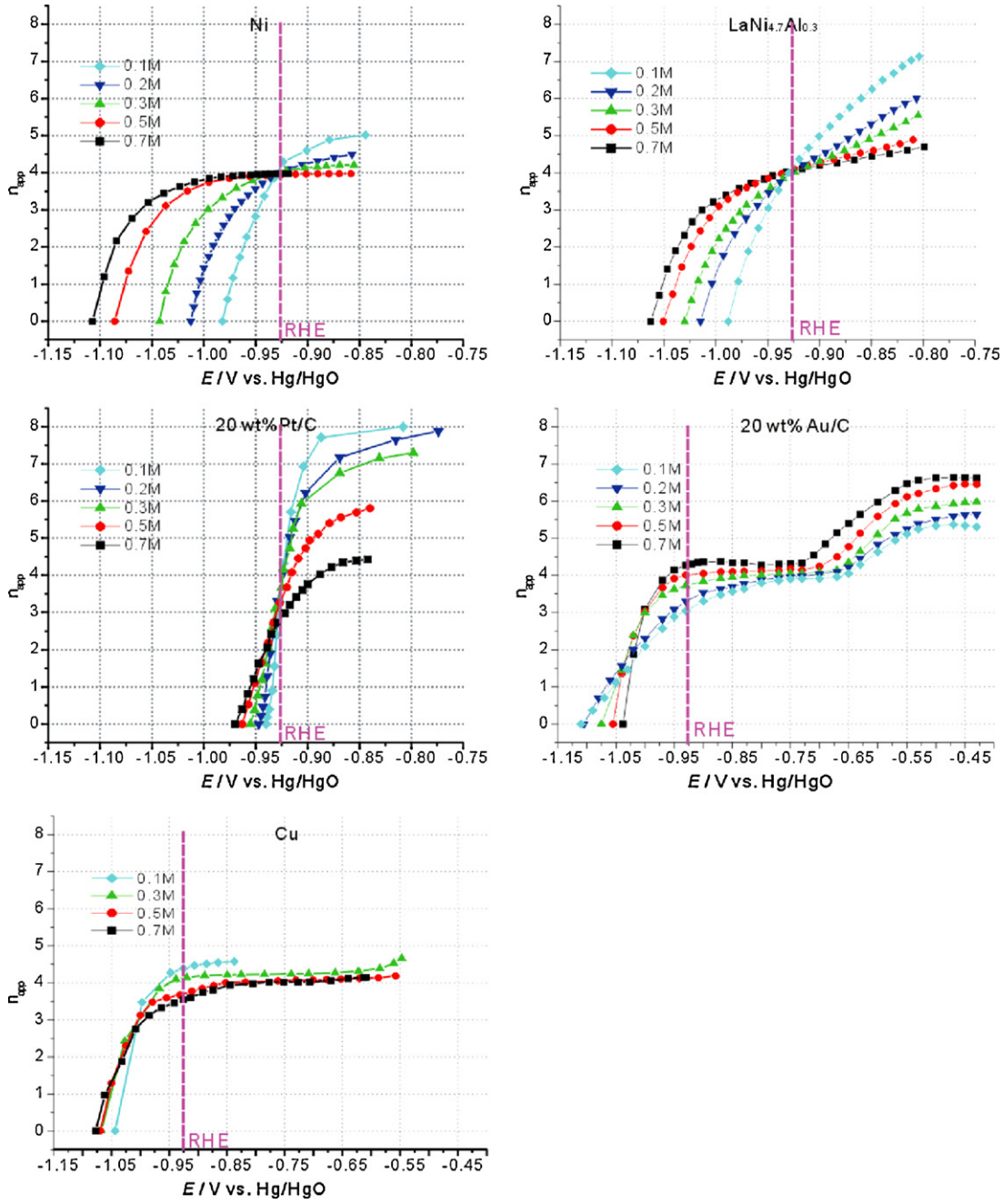

Fig. 4. n_{app} as a function of electrode potential for five tested catalysts in 2 M NaOH solution with different borohydride concentrations (data taken from Figs. 1–3).

levels off round $n_{app} = 4$ at higher borohydride concentrations. Similar situation occurs for Au/C in the potential region below −0.7 V vs. Hg/HgO. In these three cases, $n_{app} = 4$ seems to be a sort of limiting value. On the other hand, for Ni and the hydrogen storage alloy $LaNi_{4.7}Al_{0.3}$ (We tested a number of different Ni-based hydrogen storage alloys and found similar behaviors), the curve sets show a roughly common point ($E = -0.93$ V, $n_{app} = 4$). Because −0.93 V vs. Hg/HgO is the potential of RHE in alkaline solutions, the above observations strongly suggest a two-stage mechanism for borohydride oxidation: In the first stage, four H^- in BH_4^- are oxidized to four H^0 with four electrons released (Reaction (BH)); in the second stage, the H^0 is either oxidized to water (Reaction (V)) or combined to hydrogen molecules through Reaction (T) or Reaction (H). In this mechanism, H^0 is an intermediate which should be in an adsorbed state and can be denoted as H_{ads}. In the two-stage model, the reactions at a borohydride anode consist of two reaction systems, one is the four-electron oxidation of borohydride (Reaction (BH)) and the other is the hydrogen electrode reaction system (Reactions (V), (H) and (T)):

4e oxidation of borohydride $BH_4^- + 4\,OH^- \rightarrow B(OH)_4^- + 4e^- + 4H_{ads}$ (BH)

Volmer reaction $H_{ads} + OH^- \leftrightarrow H_2O + e^-$ (V)

Heyrovsky reaction $H_{ads} + H_2O + e^- \leftrightarrow H_2 + OH^-$ (H)

Tafel reaction $2H_{ads} \leftrightarrow H_2$ (T)

In contrast to the highly irreversible Reaction (BH), the hydrogen reactions are rather chemically reversible on the catalysts studied. As long as the potential is sufficiently positive, H^0, either H_{ads} or H_2, can be oxidized to water. Conversely, if the potential is

sufficiently negative, water will be reduced to H_{ads} and H_2. For ordinary hydrogen electrodes, such as a Pt electrode in hydrogen saturated solution, the dividing point between hydrogen evolution and hydrogen oxidation is the RHE in the same solution. For borohydride electrode, the situation of $n_{app} = 4$ is similar but not exactly equal to that of RHE. When $n_{app} = 4$, all the released hydrogen gas can be attributed to Reaction (BH) followed by Reaction (T), Reaction (V) and Reaction (H) are not effective in this case. The potential corresponding to $n_{app} = 4$ is not exactly at RHE (−0.93 V vs. Hg/HgO) as shown in Fig. 4, we therefore define the potential corresponding to $n_{app} = 4$ at a borohydride anode as the "pseudo reversible hydrogen electrode" potential (pRHE). In the following sections, we will discuss more about pRHE.

3.3. Current decomposition

On the basis of proposed two-stage model, the reaction rates of Reaction (BH) and the hydrogen reactions can be calculated from the simultaneous polarization-gassing measurements by Eq. (2):

$$I = i_{BH} + i_H \tag{2}$$

where I is measured current, i_{BH} is the current produced by Reaction (BH) and i_H is the current of hydrogen reactions (Reactions (V) and (H)). The anodic currents are taken as positive and anodic ones as negative. At OCP, all the electrons produced by Reaction (BH) are consumed by water reduction, therefore $I = 0$ and $i_{BH} = -i_H$. At low discharge currents, the potential is still negative to RHE so that water reduction to hydrogen occurs, i_H is negative and $I < i_{BH}$. At higher potential where hydrogen oxidation occurs, i_H is positive and $I > i_{BH}$. At sufficiently positive potentials and on highly active catalysts, all the H^0 species produced by Reaction (BH) are oxidized, resulting in $i_{BH} = i_H$ and $I = 2i_{BH}$, namely "8-electron total oxidation of borohydride".

The gas evolution is produced in principle by two sources, i.e., Reaction (BH) characterized by i_{BH} and water reduction characterized by i_H. The gas evolution rate in terms of electric current is

$$G = i_{BH} - i_H \tag{3}$$

At open circuit, $-i_H = i_{BH}$ and $G = 2i_{BH}$. In contrast, at sufficiently positive potentials where $i_{BH} = i_H$, $G = 0$. From Eqs. (2) and (3), i_{BH} and i_H can be calculated from experimentally measured I and G:

$$i_{BH} = \frac{I + G}{2} \tag{4}$$

$$i_H = \frac{I - G}{2} \tag{5}$$

The method to calculate i_{BH} and i_H from simultaneous polarization and gassing rate measurements is called the current decomposition method [15].

Because our emphasis is on the suppression of hydrogen evolution, only the i_H data are discussed in this paper. In Fig. 5, logarithm of i_H is plotted against potential E. The extrapolated potentials for $i_H = 0$ ($\log i_H \to 0$) correspond to the pRHE. Fig. 5F is the typical Tafel plot. The solid curves I_a and I_c show the measured currents, which are the algebraic sum the two internal currents i_c and i_a (dashed traces). E_{rev} is the equilibrium (reversible) potential and i_0 the exchange current. The Tafel plots of i_H deduced from current decomposition on five different anodes are similar to the typical Tafel plot, which support the current decomposition method.

The pRHE for borohydride electrodes and the RHE for ordinary hydrogen electrodes are similar but not the same. No electrochemical hydrogen reaction occurs at RHE and thus no hydrogen evolution at RHE, while at pRHE, no electrochemical hydrogen reaction occurs but there is hydrogen evolution produced by borohydride oxidation.

As shown in Fig. 5, pRHE is the dividing potential between electrochemical hydrogen oxidation to water and water reduction to hydrogen at a borohydride anode. In Fig. 5A, the pRHE is close to RHE for 0.1–0.3 M borohydride but much more positive than RHE at higher concentrations (0.5 and 0.7 M). In the latter cases the cathodic linear Tafel relationship extends to potential region obviously positive to RHE, indicating electrochemical hydrogen evolution occurs at potentials positive to RHE. This phenomenon is seemingly against the thermodynamics and was called the "underpotential hydrogen evolution" in our previous paper [19]. It was explained by assuming the presence of a high energy state of adsorbed hydrogen H^*_{ads} which is produced directly from the oxidation of H^{-1} in the borohydride anions. Fig. 5 also reveals the presence of "underpotential of hydrogen oxidation", i.e., pRHE is negative to RHE and hydrogen oxidation may occur at potentials negative to RHE (see Fig. 5D and E). In Section 3.6, a direct observation of "underpotential hydrogen oxidation" will be described and discussed.

3.4. The value of pRHE

For an ordinary hydrogen electrode, three reactions (Reactions (V), (H) and (T)) can take place at the same time, but are not equal in importance. For example, hydrogen evolution can proceed through different paths, cathodic Reaction (V) in combination with cathodic Reaction (H) (Volmer–Heyrovsky mechanism) or Reaction (T) (Volmer–Tafel mechanism), depending on nature of the catalyst. The hydrogen oxidation will follow the same mechanisms but in opposite direction. At open circuit and in a given hydrogen partial pressure, a RHE will be eventually established with a corresponding equilibrium H_{ads} activity. At RHE, there is no net hydrogen reaction and thus no external current related to the net hydrogen reaction. At the equilibrium potential, the activity of H_{ads} must automatically take a proper value so that the equilibrium potentials of the two component electrochemical reactions (Reactions (V) and (H)) are identical and equal to RHE as shown in Fig. 6A. For simplification, the exchange currents and Tafel slopes of the two component electrochemical reactions are also drawn as identical in Fig. 6A, but this simplification will not affect the discussions given below.

Unlike the ordinary RHE, the H_{ads} at pRHE is produced from borohydride oxidation (Reaction (BH)) instead of molecular H_2 adsorption or water reduction. Because of the high reducing ability of borohydride, we assume that the H_{ads} produced directly from borohydride is in a higher energy state than the equilibrium H_{ads} of ordinary RHE and denote it as H^*_{ads}. In the following paragraphs we will explain that the presence of H^*_{ads} might cause the pRHE to deviate from the RHE.

Fig. 6 illustrates a suggested model to explain the possible changes of pRHE. For the ordinary RHE, Reactions (V) and (H) have the same equilibrium potential and both are equal to the RHE (Fig. 6A). Because the H^*_{ads} has a higher energy than the H_{ads} of the ordinary RHE, the equilibrium potential of Reaction (V) ($E^*_{eq,V}$) will become negative to the RHE and that for Reaction (H) ($E^*_{eq,H}$) positive to the RHE (Fig. 6B–D). Because Reactions (V) and (H) are at the same electrode and therefore must share a common electrode potential, these two component electrochemical reactions cannot remain at their own equilibrium. The common potential under the "zero electrochemical hydrogen reaction" condition is the pRHE which must be somewhere in between $E^*_{eq,V}$ and $E^*_{eq,H}$. At pRHE, Reaction (V) has a net anodic current $I_{a,V}$ and Reaction (H) has a net cathodic current $I_{c,H}$. The two currents are equal in absolute value but opposite in direction. The total result of the two component electrochemical reactions is $2\,H^*_{ads} \to H_2$ without any external current due to the hydrogen reactions. It should be emphasized that "no external current due to electrochemical hydrogen reactions"

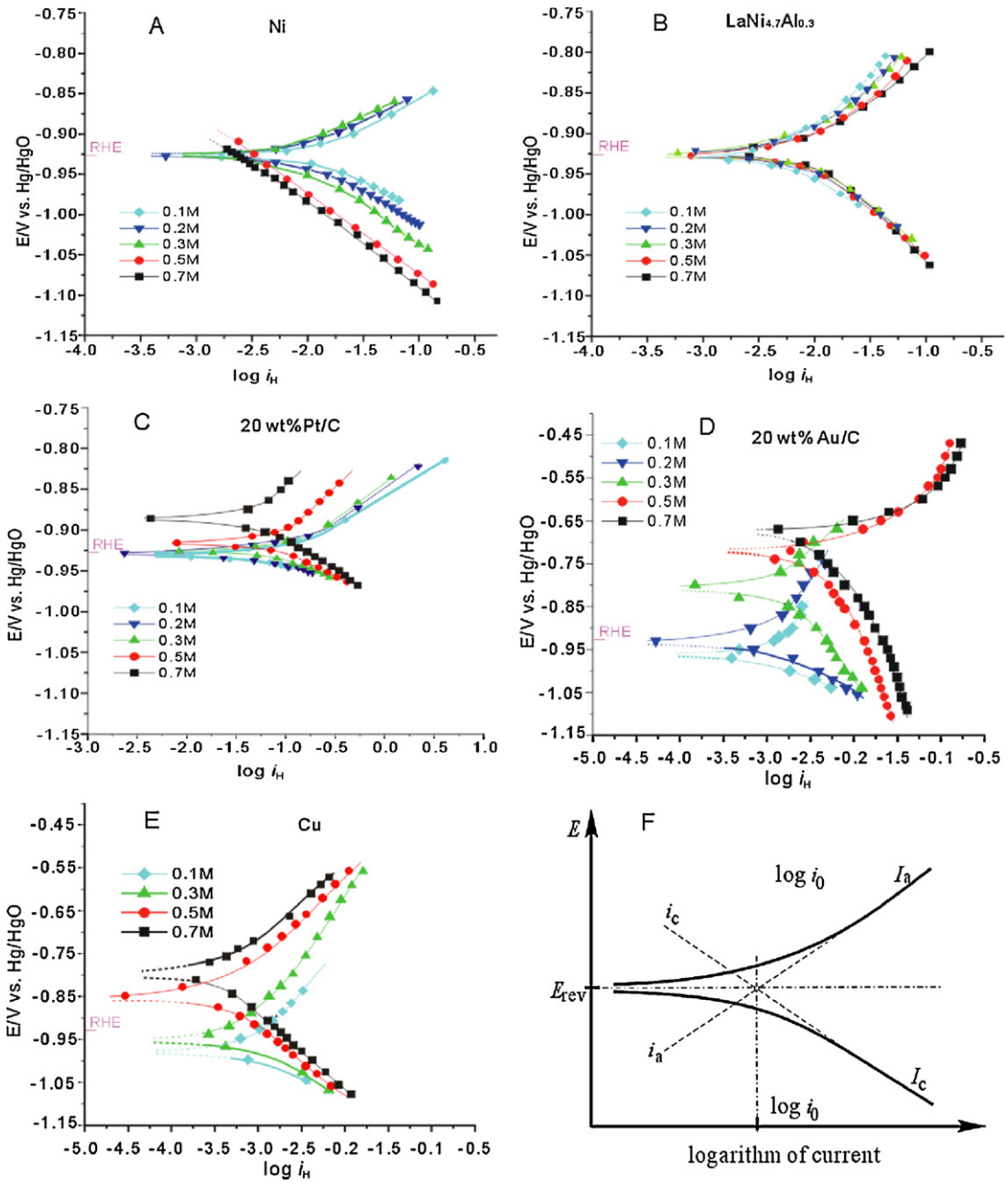

Fig. 5. Tafel plots for hydrogen reactions deduced from the current decomposition of data shown in Figs. 1–3. (F) is a general illustration of Tafel plots.

at pRHE does not necessarily mean "no external (measured) current at all". In fact, there is a current due to borohydride oxidation (Reaction (BH)).

The actual pRHE value changes with the relationship between the exchange currents of the two component hydrogen electrochemical reactions. When the two exchange currents happen to be equal, the pRHE will be the same as the RHE (Fig. 6B). When Reaction (H) has a smaller exchange current than that for Reaction (V), namely $i_{0,H} < i_{0,V}$, the pRHE will be more negative than RHE (Fig. 6C), and the opposite is true for $i_{0,H} > i_{0,V}$ (Fig. 6D).

At pRHE, $i_{a,V} = i_{c,H}$. Because of being similar to the exchange current defined in Fig. 5F, the (internal) current of electrochemical hydrogen reaction corresponding to pRHE may be called "pseudo exchange current" (pi_0).

If the hydrogen reaction follows the Volmer–Tafel mechanism, the pRHE will be determined by Reaction (V) alone and must be negative to the RHE. In our experiments it was found that the pRHE could be either negative or positive to the RHE. Therefore, the Volmer–Heyrovsky mechanism seems to be more probable than the Volmer–Tafel mechanism. It was also found in our experiments that borohydride or its boron-containing intermediates or products may adsorb strongly on catalyst surfaces. This adsorption should strongly suppress the adsorption of hydrogen, resulting in lowered surface concentrations of adsorbed hydrogen. When the coverage of adsorbed hydrogen is lowered, the probability of Reation (T) is reduced sharply. Therefore, the competitive adsorption consideration may also support the observed Volmer–Heyrovsky mechanism.

3.5. Proposed mechanistic model for borohydride anodes

Based on the above data and discussions, a mechanism for the borohydride anode is proposed as shown in Fig. 7. As for any electrode reaction, Reaction (BH) has its own equilibrium potential

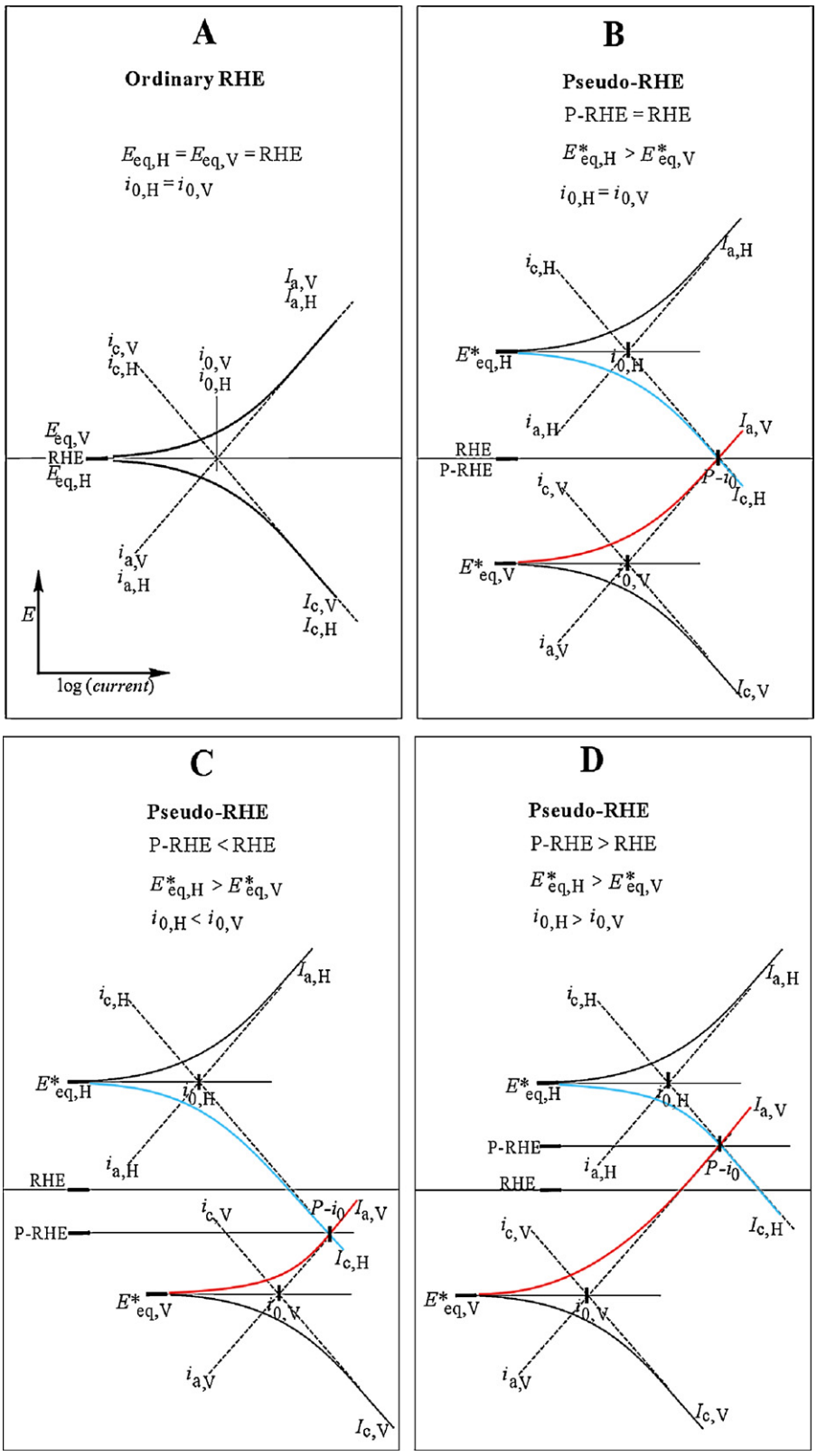

Fig. 6. Changes of pRHE with the exchange currents of component hydrogen reactions (the RHE is drawn at the same horizontal level for all four cases for easy comparison. See text for details).

$E_{eq,BH}$ but it has never been reached experimentally because of its high irreversibility. At a real borohydride anode, the actual reaction is represented by curve $I_{a,BH}$, which is the 4-electron oxidation of borohydride to form H_{ads}. In addition to the borohydride oxidation reaction, there is a hydrogen reaction system characterized by the pRHE and the pi_0 which are represented by the cross point of the cathodic curve of Reaction (H) ($I_{c,H}$) and the anodic curve of Reaction (V) ($I_{a,V}$), as explained in Fig. 6. The OCP of the borohydride anode is a mixed potential of borohydride oxidation and the hydrogen evolutions [18], as marked by the cross point L between

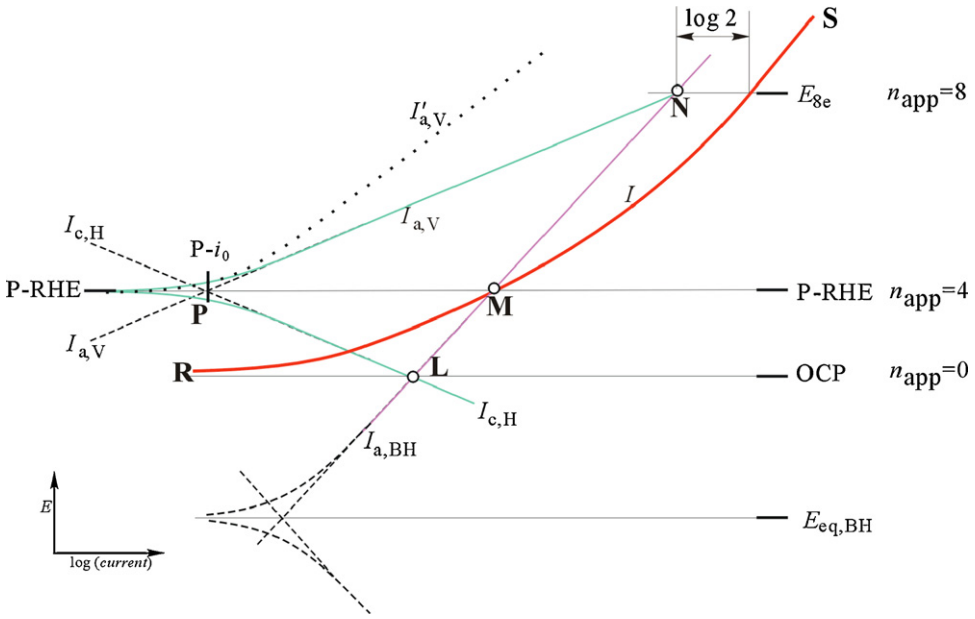

Fig. 7. Proposed mechanism for borohydride anode.

$I_{c,H}$ and $I_{a,BH}$. At OCP, all the electrons produced by Reaction (BH) are consumed by hydrogen evolution, resulting in $n_{app} = 0$ and the gas evolution rate being two times of that of Reaction (BH) alone.

The measured current I is the algebraic sum of $I_{a,BH}$ and the current due to electrochemical hydrogen reactions. At potentials between OCP and pRHE, the hydrogen current is a cathodic one, namely $I_{c,H}$, and the measured current is represented by the thick curve from point R to point M in Fig. 7. Point M corresponds to the pRHE at which the net electrochemical hydrogen reactions is zero and $I = I_{a,BH}$, $n_{app} = 4$ (refer to Fig. 4). When the potential moves up into the region between pRHE and E_{8e}, the net hydrogen electrochemical reaction is an anodic one, namely $I_{a,V}$, which is added on $I_{a,BH}$ to make $I > I_{BH}$ and $n_{app} > 4$. In this region, n_{app} increases further with potential.

If $I_{a,V}$ increases with potential faster than $I_{a,BH}$, the two relevant curves will cross to each other at a potential marked N in Fig. 7. At point N, $I_{a,V} = I_{a,BH}$ and thus $I = 2I_{a,BH}$, $n_{app} = 8$ and the corresponding potential is denoted as E_{8e}. At potentials above E_{8e}, the relationship $I_{a,V} = I_{a,BH}$ remains because the potential dependent rate constant for the anodic Reaction (V) is large enough to exhaust immediately all H_{ads} produced by Reaction (BH). As a result, the curve $I_{a,V}$ will merge with curve $I_{a,BH}$ and the horizontal distance between I and I_{BH} will be log 2 for potentials above E_{8e}. If the slope of $I_{a,V}$ is similar or even larger than $I_{a,BH}$, such as the dashed line $I'_{a,V}$, the two lines will not meet in the practically encountered potential region for a borohydride anode and $n_{app} = 8$ will never be achieved.

3.6. Attempts for 8e-oxidation below RHE

As aforementioned, to achieve higher energy efficiency in DBFC over IDBFC, E_{8e} (point N in Fig. 7) must be more negative than RHE. Therefore, the pRHE must be more negative than RHE and the pi_0 must be sufficiently large, so point N can move down, as shown in Fig. 7. The pRHE is determined by the relative values of $i_{0,H}$ and $i_{0,V}$, either decreasing $i_{0,H}$ or increasing $i_{0,V}$ or both would decrease the pRHE, but only increasing $i_{0,V}$ can increase the pi_0 at the same time (Fig. 6). Therefore, the right way to reach the goal of E_{8e} < RHE should be increasing $i_{0,V}$ (i.e., moving the line $I_{a,V}$ to the right in Fig. 7).

To the best of our knowledge, there had not been any report about increasing $i_{0,V}$ in the literature. We noted the similarity of the anode Volmer reaction with the oxidative removal of adsorbed carbon monoxide (an important reaction for methanol anode and the anode fed with CO-contaminated hydrogen): both need oxygen-containing species. It is commonly recognized that ruthenium oxides in PtRu catalyst play the role of providing active oxygen-containing surface species to speed up the removal of poisoning CO_{ads}. Therefore, it was guessed that some metal oxides may also be able to increase the $i_{0,V}$. Unfortunately, ruthenium is a very active catalyst for borohydride hydrolysis and, therefore, cannot be used as borohydride anodes. We tried other metal oxides and found an effective oxide, partially reduced titanium oxides (TiO_x), to be used as a functional support for Pt catalyst. [15] After screening Pt loadings over 5–20 wt% in Pt/TiO_x, 15 wt% was identified to be the best, with a few amount of acetylene black (AB) added to increase the necessary electric conductivity of the powder electrode. The performance of 15 wt% Pt/TiO_x-AB is shown in Fig. 8. It can be seen that for low borohydride concentrations (0.1–0.3 M) 8-electron oxidation starts at a potential more negative than the RHE, i.e., E_{8e} < RHE. The potential region between E_{8e} and RHE was called the K-region, as shown in Fig. 8 [15].

Although a K-region was obtained under the guidance of the assumption "active oxygen-containing surface species", the success is a support but not a proof for the assumption. Nevertheless, Fig. 9 seems to be well in line with the proposed mechanism in Fig. 7. Fig. 9 shows the Tafel plots of hydrogen electrode reactions for six catalysts. The three catalysts, including Ni, $LaNi_{4.7}Al_{0.3}$ and 20 wt%Pt/C, are not qualified because their pRHE values are too close to RHE. Cu and Au show pRHE values being negative to the RHE, but their pi_0 values are too small. The 15 wt% Pt/TiO_x-AB has a pRHE close to those of Cu and Au, but its pi_0 is about two orders of magnitude larger than that of Cu and Au, and thus it is able to achieve the goal of E_{8e} < RHE.

There is an interesting observation in the K-region. When the anode potential moved slowly from OCP to the positive, hydrogen evolution was fast at the beginning and then slowed down gradually. When the potential entered into the K-region, bubbling stopped. Moreover, the hydrogen bubbles originally attached on the electrode surface became smaller and eventually disappeared. It means that molecular hydrogen was oxidized at a potential more negative than the RHE, called "underpotential hydrogen oxidation". This seemingly violates the thermodynamics at a glance. How-

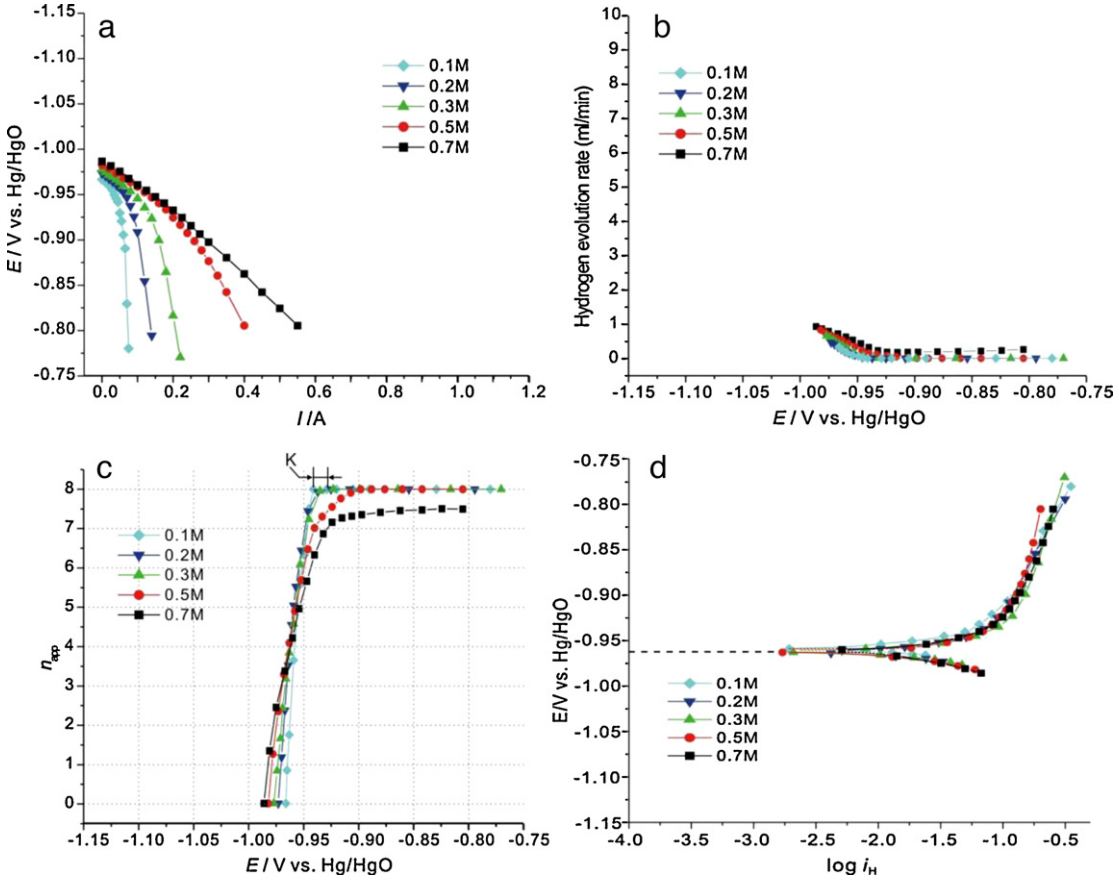

Fig. 8. Borohydride oxidation on 15 wt% Pt/TiO_x-AB in 2 M NaOH containing different concentrations of $NaBH_4$ (a) polarization curves, (b) hydrogen evolution rate, (c) n_{app} changes with potential, (d) Tafel plots of hydrogen electrode reactions obtained by current decomposition.

ever, taking into account the assumption of high energy state of H^*_{ads}, the underpotential hydrogen oxidation at 15 wt% Pt/TiO_x-AB is as understandable as the underpotential hydrogen evolution at Ni [15]. Because the K-region is above the pRHE, net electrochemical oxidation of hydrogen is feasible. The energy deficit of molecular hydrogen oxidation within the K-region is paid for by the surplus energy released on the oxidation of high energy state H^*_{ads}.

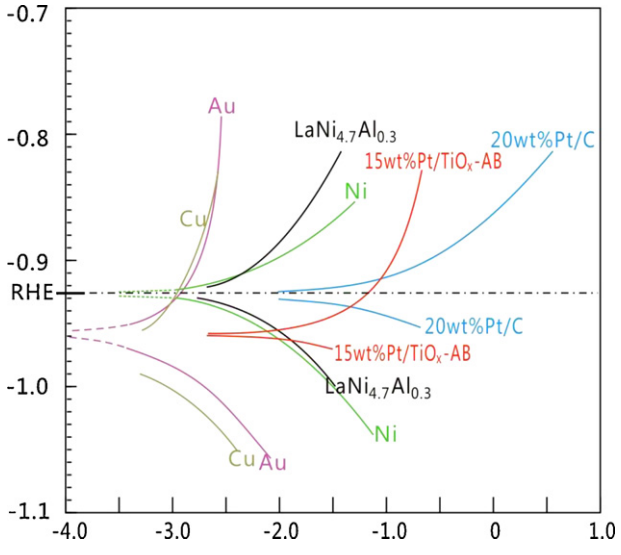

Fig. 9. Tafel plots for the hydrogen reactions on the catalysts tested in 2 M NaOH containing 0.1 M $NaBH_4$.

4. Summary

This paper provided vast systematic data with focus on the hydrogen evolution accompanying the borohydride oxidation. Based on a two-stage model of borohydride oxidation, main features of the experimental data can be rationalized, including the under-potential hydrogen evolution (hydrogen evolution at potentials positive to RHE) and the under-potential molecular hydrogen oxidation (hydrogen oxidation at potentials negative to RHE). According to the proposed mechanism of borohydride oxidation, a principle is suggested for approaching the goal of E_{8e} < RHE, which is preliminarily realized with a titanium-oxide supported Pt catalyst.

The oxidation of borohydride is a complex process. The present progress answered some questions but raised more for further studies. The two-stage model remains to be checked by more experiments. A challenging task will be the experimental verification of the proposed high energy state of adsorbed hydrogen (H^*_{ads}). From the technical point of view, the best catalyst mentioned in this paper is still not good enough. The K-region should be widened, especially in higher borohydride concentrations.

Acknowledgements

This work was financially supported by the Natural Science Foundation of China (grant no. 20933004, 20773096 and J0730426), the National Hi-Tech R&D Program (grant no. 2007AA05Z142) and the Fundamental Research Funds for the Central Universities

(203275662, 203275672). We thank Dr. Kai Jiang for providing the TiO_x sample and Prof. Chuan-Sin Cha and Prof. George Chen for helpful discussions.

References

[1] S.C. Amendola, S.L. Sharp-Goldman, M.S. Janjua, N.C. Spencer, M.T. Kelly, P.J. Petillo, M. Binder, A. Safe, Portable, Int. J. Hydrogen Energy 25 (2000) 969.
[2] M.E. Indig, R.N. Snyder, J. Electrochem. Soc. 109 (1962) 1104.
[3] R. Jasinski, Electrochem. Technol. 3 (1965) 40.
[4] S.C. Amendola, P. Onnerud, M.T. Kelly, P.J. Petillo, S.L. Sharp-Goldman, M. Binder, J. Power Sources 84 (1999) 130.
[5] J.H. Kim, H.S. Kim, Y.M. Kang, M.S. Song, S. Rajendran, S.C. Han, D.H. Jung, J.Y. Lee, J. Electrochem. Soc. 151 (2004) A1039.
[6] B.H. Liu, Z.P. Li, J. Power Sources 187 (2009) 291.
[7] J. Ma, N.A. Choudhury, Y. Sahai, Renew. Sustain. Energy Rev. 14 (2010) 183.
[8] C. Ponce de Leon, F.C. Walsh, D. Pletcher, D.J. Browning, J.B. Lakeman, J. Power Sources 155 (2006) 172.
[9] J. Ma, Y. Sahai, R.G. Buchheit, J. Power Sources 195 (2010) 4709.
[10] J.P. Elder, A. Hickling, Trans. Faraday Soc. 58 (1962) 1852.
[11] E. Gyenge, Electrochim. Acta 49 (2004) 965.
[12] C. Celik, F.G. Boyaci San, H.L. Sarac, Int. J. Hydrogen Energy 35 (2010) 8678.
[13] J.I. Martins, M.C. Nunes, R. Koch, L. Martins, M. Bazzaoui, Electrochim. Acta 52 (2007) 6443.
[14] R. Jamard, A. Latour, J. Salomon, P. Capron, A. Martinent-Beaumont, J. Power Sources 176 (2008) 287.
[15] K. Wang, J. Lu, L. Zhuang, J. Phys. Chem. C 111 (2007) 7456.
[16] S. Lu, J. Pan, A. Huang, L. Zhuang, J. Lu, Proc. Natl. Acad. Sci. U.S.A. 105 (2008) 20611.
[17] B. Yang, Q. Lu, Y. Wang, L. Zhuang, J. Lu, P. Liu, Chem. Mater. 15 (2003) 3552.
[18] B.H. Liu, Z.P. Li, S. Suda, J. Electrochem. Soc. 150 (2003) A398.
[19] K. Wang, K. Jiang, J. Lu, L. Zhuang, J. Power Sources 185 (2008) 892.